Available online at www.sciencedirect.com
SCIENCE DIRECT®
Carbohydrate Research 339 (2004) 2683–2691
Carbohydrate RESEARCH

Structural parameters of amylopectin clusters and semi-crystalline growth rings in wheat starches with different amylose content

Vladimir P. Yuryev,[a,*] Alexei V. Krivandin,[a] Valentina I. Kiseleva,[a] Lyubov A. Wasserman,[a] Natalia K. Genkina,[a] Jozef Fornal,[b] Wioletta Blaszczak[b] and Alberto Schiraldi[c]

[a]*Institute of Biochemical Physics, Russian Academy of Sciences, Kosygina Str. 4, 119991 Moscow, Russia*
[b]*Institute of Animal Reproduction and Food Research, Polish Academy of Sciences, Olsztyn, Tuwina 10, 10-747, Poland*
[c]*DISTAM, University of Milan, via Celoria 2, 20133, Milan, Italy*

Received 13 May 2004; received in revised form 3 September 2004; accepted 7 September 2004
Available online 14 October 2004

Abstract—Small-angle X-ray scattering (SAXS) and scanning electron microscopy (SEM) were used to investigate the internal structure of wheat starch granules with different amylose content. Different approaches were used for treatment (interpretation) of SAXS data to assess the values of structural parameters of amylopectin clusters and the size of crystalline and amorphous lamella in different wheat starches. The average values of the semi-crystalline growth rings thickness in starches have been determined and the relationship between structural characteristics and thermodynamic melting parameters is discussed.

Keywords: Wheat starch; Amylose content; Growth rings; Amylopectin clusters; Lamellar structure

1. Introduction

A structural periodicity was recognized in semi-crystalline starch granules as alternating layers of crystalline and amorphous lamellae called clusters.[1,2] About 10 such clusters form a 100 nm thick semi-crystalline growth ring.[3] For waxy (amylopectin) and normal native starches the overall thickness of the cluster is approximately 9–10 nm[4–7] and that for the crystalline lamella is 5–6 nm.[8] The crystalline lamella is believed to consist of ordered double helices mainly formed by amylopectin A-chains and amylose tie-chains.[1,2,8,9] The latter term ('tie-chains') implies only the portions of macromolecules that connect with crystalline lamella and have elongated (straightened) conformations inside crystalline lamellae and an unordered conformation after extending from crystalline to amorphous lamellae.[1,2,8,9] This corresponds to the absence of any orientation of tie-chains within amorphous lamellae and their 'hard, longitudinal' orientation inside crystalline lamellae. Beside tie-chains the amorphous lamella consists of amylopectin B-chains.[1,2,6,7] These investigations have been extended to maize, pea, and barley starches, which have larger amylose content, and these studies revealed an increased thickness of crystalline lamellae, although with the same overall thickness of each cluster.[5] However, for the new mutant wheat starches (amylopectin and high amylose starches) that have been produced in the middle of the 1990's and at the beginning of this century,[10–12] little data are currently available regarding the effects of amylose content on the structure of the clusters as well as on the sizes of semi-crystalline growth rings.

To date, the study of native wheat starches containing from 1.5% to 39.5% amylose has shown that in spite of

* Corresponding author. Tel.: +7 095 939 74 42; fax: +7 095 137 41 01; e-mail: v.yuryev@sky.chph.ras.ru

0008-6215/$ - see front matter © 2004 Elsevier Ltd. All rights reserved.
doi:10.1016/j.carres.2004.09.005

changes in amylose content, both A-type polymorphous structure in native granules and the thickness of crystalline lamella (4.7 ± 0.5 nm) remain unchanged.[12] At the same time, in going from amylopectin to high amylose starches, a decrease of the degree of crystallinity has been observed.[12] In this respect, the bimodal starches from wheat and barley show reasonably similar behavior.[12,13] There are two populations of size distribution in granules of bimodal starches. For example, for wheat starches the size of the small granules is below 10–14 μm while the size of the large granules ranges between 10–14 μm and 36 μm. In contrast, in monomodal starches, for instance those from maize and pea,[14,15] only one granule population size distribution is observed. For the starches from latter two varieties, changes in polymorphous structure and increased thickness of crystalline lamellae are observed when passing from amylopectin (waxy) to high amylose starches.[5,8,14,15] Consequently, the direct application of already existing information about 'traditional' starches from different crops to relatively unstudied mutant wheats may be rather unreliable. The assessment of the cluster size in mutant wheat starches is important to define their structural features and to obtain a better understanding of the relationship between sub- and supra-molecular structures and their thermodynamic melting parameters. The results of a study on the thermodynamic properties of mutant wheat starches have been recently published.[12] In that paper it was proposed that the observed decrease in the melting temperature with increasing amylose content could be due to accumulation of defects in the granule structure.

Small-angle X-ray scattering (SAXS) and neutron scattering patterns from starch samples show a broad diffraction peak related to the periodical arrangement of the clusters in the semi-crystalline granules. The thickness of the cluster (the overall thickness of one crystal plus one amorphous lamella) can be calculated from the position of this peak by applying the Wolf–Bragg equation or through the paracrystalline diffraction theory. The application of Wolf–Bragg equation is straightforward but the value of the cluster size determined by this method can differ slightly from the correct one. The paracrystalline diffraction method is more sophisticated and is more physically meaningful because it takes into account the nonideal periodicity of clusters in semi-crystalline growth rings. In addition to providing the cluster size, this method also yields a great deal of other information about the structure of native starches.[3–7] However, the paracrystalline method involves fitting many structural parameters, the evaluation of which may be ambiguous. Moreover, the results obtained by this method depend on the type of paracrystalline model chosen.

Information about higher-level structural organization in starch polysaccharides, like semi-crystalline growth rings, can be drawn from various microscopy approaches. Growth rings of potato starch are visible by means of light microscopy without any previous treatment while those for other starches[16–18] require application of atomic force microscopy. Those for wheat starch can be visualized with scanning electron microscopy (SEM) after previous enzymatic or acid treatment.[16] Computer-assisted analysis of SEM data allows the quantitative characterization of the semi-crystalline growth rings.

In this work, we used SAXS and SEM investigations to probe the effect of amylose content in mutant wheat starches on the structural parameters of amylopectin clusters. The SAXS data were processed both with the Wolf–Bragg equation and with the paracrystalline diffraction method. To provide a more detailed picture of the clusters, we compared the results of the studies reported here with studies using wide-angle X-ray scattering (WAXS) and differential scanning calorimetry (DSC), which have previously been published.[12]

2. Materials and methods

2.1. Materials

Different wheat varieties were selected through chemical mutagenesis, using ethylene-imine as the mutagen.[19] The wheat cultivars investigated were grown in central Russia (Moscow Region) in the 2000 growing season.

Native starches were isolated according to Richter et al.[20] The starch from wheat variety 'Leona' was kindly supplied by Dr. P. Seib. The moisture content in the starches studied was in the range of 11–12%. Characteristics of native starches and the methods of their determination were published elsewhere[12] and some of them are presented in Table 1.

Table 1. Some characteristics of wheat starches[12]

Wheat varieties	Amylose content[a] (%)	Degree of crystallinity, DC_{WAXS}[b] (%)	L_{crl}[c] (nm)	$T_{m\,crl}$[d] (K)
Leona	1.5	30	4.5 ± 0.4	336.6 ± 0.2
Beseda	11.2	25	4.5 ± 0.2	331.3 ± 0.1
Im. Rapoporta	26.0	—	4.9 ± 0.2	330.5 ± 0.1
Bulava	39.5	23	4.2 ± 0.2	329.7 ± 0.1

[a] The amylose content in the samples was determined spectrophotometrically using iodine complexation.[20]

[b] The degree of crystallinity of native starches (DC_{WAXS}) was determined from WAXS data using ball-milled wheat starch as an 'amorphous' standard.

[c] The thickness of crystalline lamellae was determined using the 'two-state' model applied for description of the melting process of native starches.

[d] The peak melting temperature of crystalline lamellae.

2.2. Methods

2.2.1. Small-angle X-ray scattering (SAXS). For SAXS measurements, powders of native starches were dispersed in an excess of distilled water to form slurries with ~50% weight fraction of dry matter, as described previously.[4,5]

SAXS measurements were carried out in transmission geometry using an X-ray diffractometer designed in the Institute of Biochemical Physics (Moscow, Russian Federation). During X-ray exposure, the starch slurries were kept in sealed cells to prevent dehydration. The X-ray beam emitted from the fine-focus Cu X-ray tube operating at 30 kV/30 mA was Ni-filtered and line-focused with a glass mirror (Franks-type collimator[21]). The SAXS patterns were recorded with a gas-filled (85% Xe, 15% Me) one-dimensional position-sensitive detector[22] with a delay line readout constructed in the Joint Institute for Nuclear Research (Dubna, Moscow Region, Russian Federation). The sample-to-detector distance was 415 mm. Experimental SAXS curves were corrected for the background scattering, corrected for collimation distortions (desmeared) as reported[23] and plotted as a function of $S = (2\sin\theta)/\lambda$, λ and θ being the CuK_α-wavelength (0.1542 nm) and half the scattering angle, respectively. Collimation correction was performed with the SAXS data processing program PRO, developed in the Institute of Crystallography (Moscow, Russian Federation). Curve fitting for the desmeared SAXS curves was performed with the curve fitting procedure in the program package EasyPlot for Windows ver.2.22-5 (Spiral Software & MIT).

Parameters of the SAXS peaks (intensity I_{max}, position S_{max}, and full width at half maximum ΔS) were determined by the simple graphical method as shown for one starch sample in Figure 1. These parameters were also obtained by fitting the SAXS curves to the equation:

$$I(S) = I_{max}[1 + (2(S - S_{max})/\Delta S)^2]^{-1} + aS^{-x}, \quad (1)$$

where I_{max}, S_{max}, ΔS, a, and x are positive adjustable parameters. The first term in Eq. 1 is given by the Cauchy function and describes the SAXS peak. The second term is given by the power-law function and describes the underlying diffusive scattering. The example of a fit of SAXS curve by this method and its resulting decomposition into diffraction peak and underlying diffusive scattering is shown in Figure 2. The Bragg spacing D was calculated according to the Wolf–Bragg equation as $D = (S_{max})^{-1}$.

The SAXS curves were also analyzed according to paracrystalline diffraction theory.[24–26] It was assumed that a cross-section of all crystalline lamellae has the same single step function for the electron density profile of width L, and that paracrystalline lattice distortions arise from a variation of the thickness of the amorphous layers separating crystalline lamellae. The SAXS intensity was assumed to be the sum of the paracrystalline diffraction term $A{\cdot}S^{-1}{\cdot}f^2{\cdot}S{\cdot}Z(S)$ and the additional scattering component $aS^{-x} + k$:

$$I(S) = AS^{-1}f^2(S)Z(S) + aS^{-x} + k. \quad (2)$$

In this expression, A and S^{-1} are a scaling factor and the inverse Lorentz correction factor, respectively, and $f(S)$ is the scattering amplitude for a single crystalline lamella of thickness L,

$$f(S) = \frac{\sin(\pi LS)}{\pi S}, \quad (3)$$

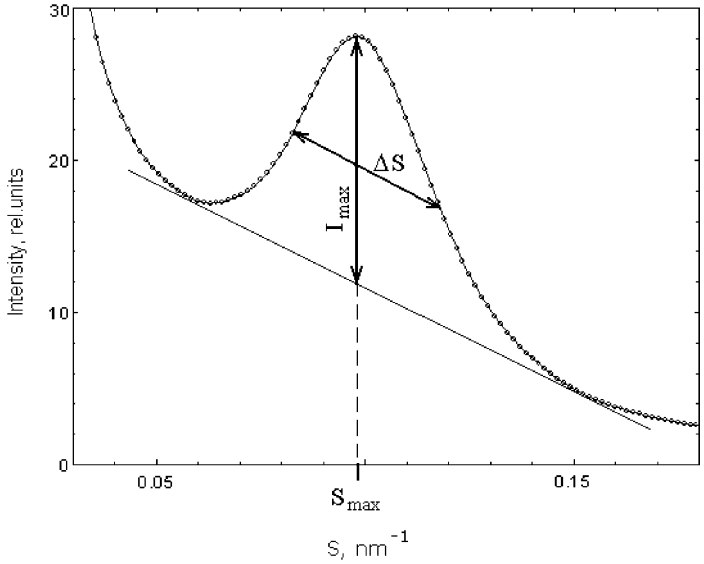

Figure 1. Desmeared SAXS pattern of Leona amylopectin wheat starch slurry and a sketch of the graphic determination of the SAXS maximum position (S_{max}), intensity (I_{max}), and full width at half maximum (ΔS).

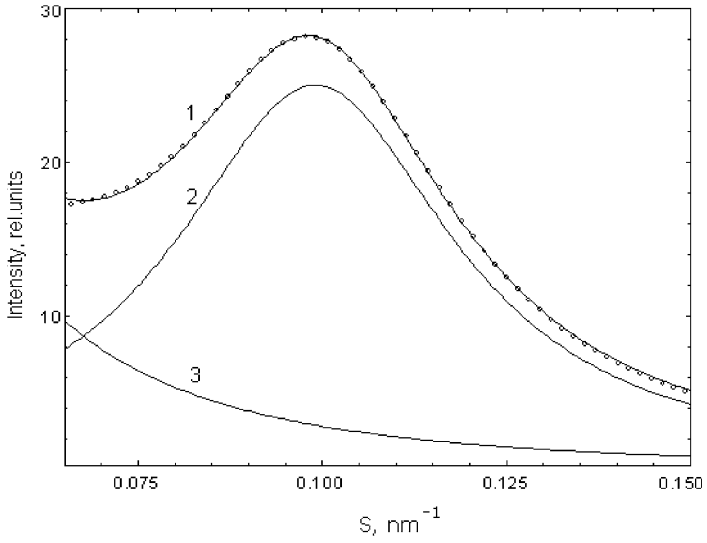

Figure 2. The desmeared SAXS pattern of Leona amylopectin wheat starch slurry (1, open circles) and its fit (1, line) by the sum of the diffraction peak (2) and power-law diffusive scattering (3) according to the Eq. 1.

and $Z(S)$ is the interference function (lattice factor),[25]

$$Z(S) = \frac{1 - |F(S)|^2}{1 - 2|F(S)|\cos(2\pi S\bar{\alpha}) + |F(S)|^2}. \quad (4)$$

In Eq. 4 $F(S)$ is the Fourier transform of the distance distribution function $H_1(x)$ for the centers of adjacent crystalline lamellae, and $\bar{\alpha}$ is the average distance between the centers of such lamellae, that is, the average thickness of the amylopectin cluster. To evaluate $F(S)$ we assumed, as described previously,[24,25] that $H_1(x)$ follows the normal Gaussian law with a mean square deviation σ:

$$H_1(x) = \frac{1}{\sigma\sqrt{2\pi}} \exp\left(-\frac{(x+\bar{\alpha})^2}{2\sigma^2}\right) \quad (5)$$

The SAXS intensities were fitted for $0.017 < S < 0.2$ with the expression 2 with A, a, x, k, L, $\bar{\alpha}$, and σ as variables and the paracrystalline structure parameters L, $\bar{\alpha}$, and σ for the starch semi-crystalline growth rings were determined as described. An example of such a fit for one of the starch samples studied is shown in Figure 3.

2.2.2. Scanning electron microscopy (SEM). Native starch granules were treated in hydrochloric acid solution[27] before SEM investigations. Briefly, 50 mg (d.w.) starch granules were exposed to the action of 3 mL of 8% (2.2 N) hydrochloric acid in a tightly sealed 30 mL centrifuge tube. The tube was continuously and gently shaken in a water bath at 38 °C for 12 h. After addition of 15–20 mL of cold distilled water, the tubes were centrifuged. The supernatant was discarded and the starch residue (a pellet) was washed with water to neutral pH and dried in an oven at 25 °C.

The granular morphology of starches was studied with SEM. The starch sample was fixed upon a gold-coated specimen holder (a two-side adhesive copper plate), in a vacuum evaporator (Jeol JEE 44E) and analyzed with a scanning electron microscope (Jeol JSM 5200) under a 10 kV potential drop.

2.2.3. Digital image analysis (DIA) of granules morphology. SEM photographs (12.2 cm × 8.7 cm) of starch at the same magnification (5000×) were scanned with an Epson Expression 1680 Pro scanner connected with PC Pentium 4 computer working in a MS-Windows environment. The resolution was set at 800 dpi resolution and the images were saved in as 256 gray level TIF files. The scanning program Adobe Photoshop 5.LE was used. Acquired images were analyzed and processed using the Olympus Micro Image 4 (Olympus Europe) software package. A previous calibration was performed using a picture scaling bar. The parameters of the semi-crystalline growth rings were measured using digital image analysis (DIA). DIA was performed using Olympus Micro Image 4 (Olympus Europe) on software designed for the automated measurement of characteristic profiles from the photographs. The characteristic measured in the work presented here was the thickness of semi-crystalline rings using the standard procedure (gray level) after enhancing sharpness, brightness, and contrast.

Because the interiors of the granules were photographed at different angles, only some of the many images were chosen for analysis. In particular, the analysis was done on those with the most planar chip surface and the most parallel orientation of this surface toward part of the specimens. The thickness of each semi-crystalline ring was measured at more than 40 points along its length, which gives 200–280 results for all specimens analyzed for each starch sample. For each starch sample, five to seven SEM photographs were examined.

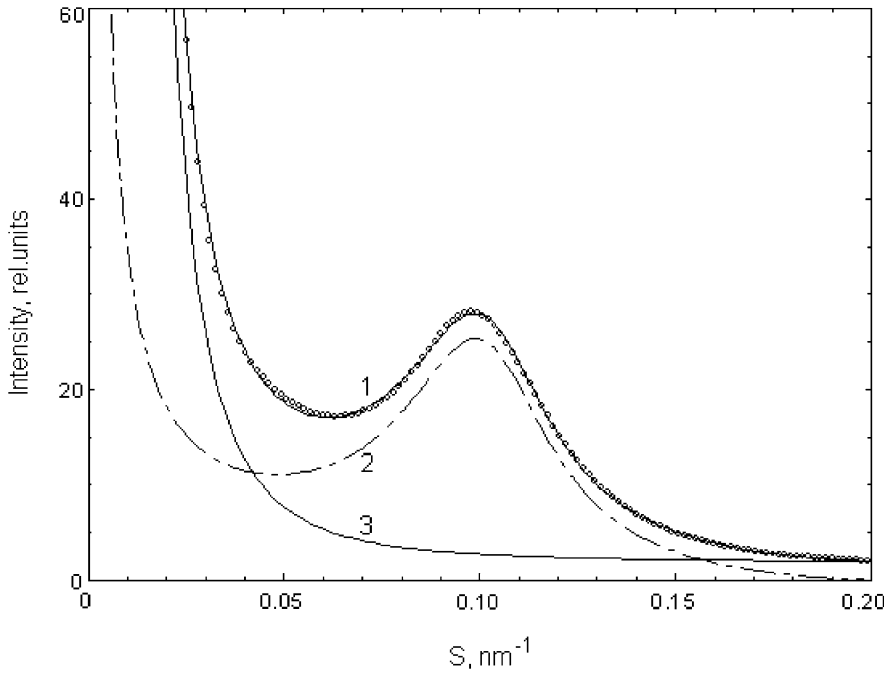

Figure 3. Desmeared SAXS pattern of Leona amylopectin wheat starch slurry (1, open cirlces) and its fit (1, line) according to the expression 2 by the sum of the paracrystalline diffraction term (2) and additional scattering component (3).

3. Results and discussion

The SAXS patterns of the starches studied are shown in Figure 4, which are at the same relative scale and therefore directly comparable. It is evident from the figure that the diffraction intensity from amylopectin starch is about three times higher in comparison with the values for the other starches. The SAXS-derived parameters of the amylopectin clusters are presented in Tables 2–4.

Table 2 contains the data obtained by graphical analysis of the SAXS peak and through the Wolf–Bragg equation. Table 3 contains the data obtained by the analytical treatment of the SAXS peak and the Wolf–Bragg

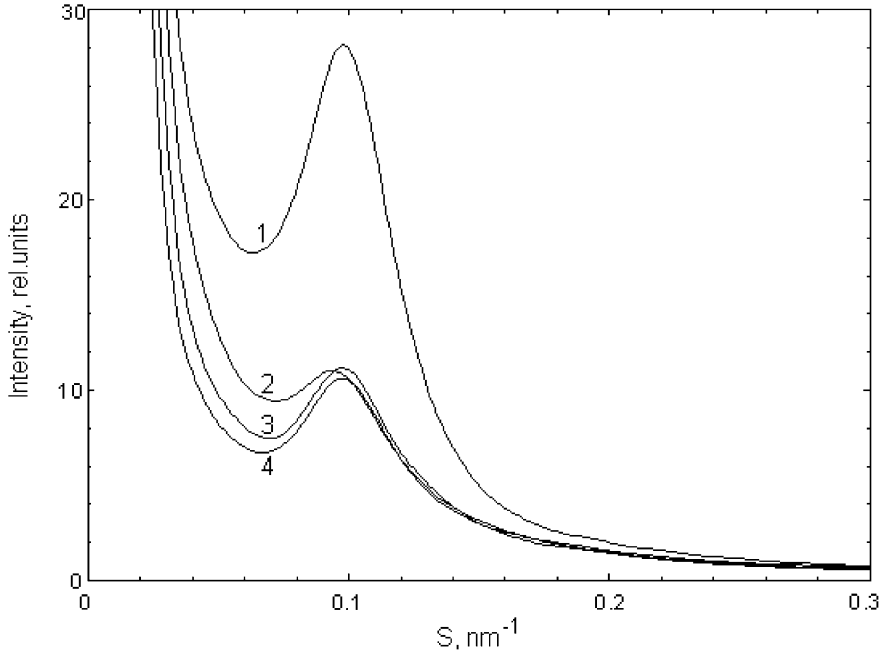

Figure 4. Desmeared SAXS patterns of the wet wheat starch slurries (1—Leona, 2—Bulava, 3—Beseda, 4 — Im. Rapoporta varieties).

Table 2. Intensity (I_{max}), position (S_{max}), full width at half maximum (ΔS), and Bragg spacing ($D = (S_{max})^{-1}$) of the SAXS maximum for the wet starches, determined as shown in Figure 1[a]

Starch	I_{max} (rel. units)	S_{max} (nm^{-1})	ΔS (nm^{-1})	D (nm)
Leona (1.5% amylose)	16.2	0.098	0.037	10.2
Beseda (11.2% amylose)	5.5	0.098	0.036	10.2
Im. Rapoporta (26.0% amylose)	5.5	0.098	0.036	10.2
Bulava (39.5% amylose)	3.8	0.094	0.036	10.6

[a] The accuracy in the measurement is $\pm 0.001\,nm^{-1}$ for S_{max} and ΔS and ± 0.2 rel. units for I_{max}.

Table 3. Intensity (I_{max}), position (S_{max}), full width at half maximum (ΔS), and Bragg spacing ($D = (S_{max})^{-1}$) of the SAXS maximum for the wet starches, determined from the results of the least squares fit according to Eq. 1 as depicted in Figure 2

Starch	I_{max} (rel. units)	S_{max} (nm^{-1})	ΔS (nm^{-1})	D (nm)
Leona (1.5% amylose)	25.3	0.099	0.046	10.1
Beseda (11.2% amylose)	8.1	0.099	0.044	10.1
Im. Rapoporta (26.0% amylose)	7.9	0.099	0.044	10.1
Bulava (39.5% amylose)	7.7	0.096	0.053	10.4

Table 4. Parameters of the lamellar structure: average repeat distance $\bar{\alpha}$ corresponding to thickness of amylopectin clusters, its mean square deviation σ, and crystalline lamella thickness L_{crl} found for the starch granules according to the paracrystalline diffraction theory

Starch	$\bar{\alpha}$ (nm)	σ (nm)	L_{crl} (nm)
Leona (1.5% amylose)	8.9	2.6	4.8
Beseda (11.2% amylose)	8.8	2.6	4.6
Im. Rapoporta (26.0% amylose)	8.8	2.6	4.6
Bulava (39.5% amylose)	8.5	2.8	4.9

Obtained by a least-squares fit of the experimental intensity with Eq. (2) for $0.017 < S < 0.2$.

equation. Table 4 shows the results of the SAXS curves processed according to paracrystalline diffraction theory.

The analysis of the data presented shows that, irrespective of the method of determination, the changes in the calculated parameters observed with increasing amylose content are rather similar. The values obtained are in agreement with results published for normal wheat[7] and some other starches.[3–6,28] However, it is worth noting that the average repeat distance $\bar{\alpha}$ determined by the paracrystalline approach (Table 4) is about 10% smaller than the Bragg distance D (Tables 2 and 3), and this is in agreement with results reported by others.[4]

As can be seen from Tables 2 and 3 and Figure 4, an increase in amylose content leads to a 3–4-fold decrease in the intensity of the scattering maximum (I_{max}). According to X-ray diffraction theory,[24–26] I_{max} depends on the amount of the ordered semi-crystalline structures and/or on the differences in electron density between crystalline and amorphous lamellae in given starches. Because the degree of crystallinity in starches studied varies insignificantly (Table 1), it can be postulated that the observed changes in I_{max} mainly reflect the difference in the electron density between crystalline and amorphous lamella.

Three hypotheses can be proposed to explain the decrease in the differences in electronic density between crystalline and amorphous lamellae on increasing amylose content in native starches. Namely: (i) co-crystallization of amylose macromolecules with amylopectin A-chains,[5] (ii) accumulation of amylose chains oriented transversely to the lamella stack within amorphous lamellae,[29] (iii) accumulation of amylose tie-chains oriented along lamella stack inside both crystalline and amorphous lamellae.[8,30–32]

Each hypothesis was considered using the Thomson–Gibbs' equation[33]

$$T_m = T^\circ_m[1 - 2\gamma_i/(\Delta H^\circ_m \rho_{crl} L_{crl})]$$

where T°_m and H°_m are the melting temperature and the melting enthalpy, respectively, of a hypothetical crystal with unlimited size (a perfect crystal). γ_i is the free surface energy of face sides of crystalline lamellae, while ρ_{crl} and L_{crl} are, respectively, the density and the thickness of the crystal, for semi-crystalline polymers[33] and starches.[8,32] Our analysis is based on the thesis that there is a relationship between structure and thermodynamic properties for bio- and synthetic polymers.

The following was considered in the analysis: (i) amylose and amylopectin macromolecules are incompatible in solution[34] and gels,[35] (ii) water content in wheat seeds during their ripening is changed from 80% to 18%,[36] and (iii) most of the ordered structures are formed up to milky-waxy or waxy ripening stages for wheat[32,37] and wrinkled pea[30,32] when water content reaches approximately 40%, for wheat seeds.[36] In particular, it is difficult to imagine conditions that would allow for co-crystallization of amylose and amylopectin macromolecules. Additionally, if an increase in the thickness of crystalline lamellae truly exists over all ranges of amylose content (from 0% to 70%),[5] we should observe[33] an increase in T_m values. However, analysis of published data on changes in T_m values for wheat, barley, and maize starches,[12,38,39] containing from 1% to 39.5% amylose, shows a decrease or an invariability in T_m

value with increasing amylose content. This temperature 'jump' in T_m has been observed only for maize starches[8,39] containing 50% and 70% amylose. In this case, the thickness of crystalline lamellae, estimated both from DSC and SAXS data is indeed in the range of 7.2–9.1 nm.[5,8,30]

It is well known that melting of crystals begins from their defects.[40] According to Gidley,[29] the localization of amylose chains in amorphous lamellae realizes in more and more degree at a passing from amylopectin to high amylose starches. Such chains cannot be considered as crystalline phase defects and, correspondingly, they do not affect the melting temperature of crystals.

In the contrast to previous conclusions, amylose tie-chains can be considered as defects located both in crystalline and amorphous lamellae. An accumulation of such chains is observed both at passing from amylopectin to high amylose starches containing <50% amylose and at structure formation of native granules during their biosynthesis. These phenomena are usually accompanied by a decrease in T_m of starches. It is proposed that a temperature 'jump' in starches containing $\geqslant$50% amylose is the result of the formation of amylose double helices from amylose tie-chains when the content of these chains in granules reaches the critical magnitude.[8,32] As amylose content in native wheat starches does not exceed 39.5%, it could be expected that an increase of amylose in wheat starches would be accompanied by decreasing T_m values. Such changes have been observed[12] (Table 1) for the starches studied here. The accumulation of defects formed from amylose tie-chains could be sufficient explanation for the decreasing differences in electronic density between crystalline and amorphous lamellae at passing from amylopectin to high amylose wheat starches containing $\leqslant$50% amylose. In this case, it can be concluded that amylose tie-chains act as defects in crystalline lamellae, decreasing their density and simultaneously increasing the molecular density of amorphous lamellae.

In summary, it can be concluded that a decrease of electronic density between crystalline and amorphous lamellae in wheat starches is due to an accumulation of amylose tie-chains with increasing amylose content in the granules.

It could be expected that an accumulation of defects, in particular, amylose tie-chains, can lead to the changes of the size or clusters as a whole or the sizes of both lamellae with an unchanged overall cluster size. A solution to this problem is of interest for two reasons: (i) such data are absent for mutant wheat starches and (ii) a decrease in T_m at increasing amylose content in wheat starches (Table 2) can be both due to increasing content of amylose tie-chains and the changes of crystalline lamellae thickness.

The data from Tables 2 and 3 allow for the possibility that the overall thickness of clusters in amylopectin and normal wheat starches is constant, while a slight increase (in average of 0.3–0.4 nm) of the cluster size possibly takes place on passing from normal to high amylose wheat starches. However, the latter conclusion is not supported by the results obtained from the application of the paracrystalline diffraction theory (Table 4), as well as by the results of the work[5] on maize, pea, and barley starches. According to the data from Table 4 and previous studies,[5] the overall thickness of clusters is constant irrespective of the amylose content.

The values of the thickness of the crystalline lamellae drawn from SAXS data according to the paracrystalline model (Table 4) are very close to each other and to those obtained from DSC investigations using the 'two-state' model of the melting transition (Table 1 reports the data only for four of seven wheat starches[12] with different amylose content). Moreover, the estimations of L_{crl} obtained from SAXS (Table 4) and DSC (Table 1)[12] measurements show that irrespective of amylose content in wheat starches, L_{crl} is constant. It follows that joint SAXS and DSC data confirm the thesis that there is a relationship between structure of starches and their thermodynamic properties. On the other hand, this conclusion is not supported by the data reported previously.[5] In that work, the authors concluded that the increase of amylose content leads to an increase of the thickness of the crystalline lamellae in legumes and maize samples containing $\geqslant$50% amylose.[30,39] It cannot be excluded that these discrepancies may be due to differences in the amylose content of the starches investigated in the study[30,39] and in the present paper.

From the analysis using the Thomson–Gibbs equation, it can be concluded that a lower melting temperature is related to the changes of three parameters: the polymorphous structure of the crystal, the thickness, and the surface free energy of crystals. Because an increase of amylose content in wheat starches does not imply a change in their polymorphous structure[12] nor thickness of crystalline lamella (Table 1[12] and Table 4), the main contribution to T_m changes comes from the changes in surface free energy of crystals. This, in turn,[33] is mainly dependent on surface entropy, which is proportional to the content of defects. Therefore, an increase in defects may produce a decrease of the melting temperature of the crystals.[32] The analysis of SAXS and DSC data suggests that the main reason for a lower melting temperature in wheat starches is apparently an accumulation of defects with increasing amylose content.

It is well known[1–5] that semi-crystalline growth rings consist of amylopectin clusters. Therefore it was of interest to determine the influence of amylose content on sizes of semi-crystalline growth rings, as such data are lacking for wheat mutant starches. SEM photographs of wheat starches are presented in Figure 5. Alternating light and dark layers are observed, the former being

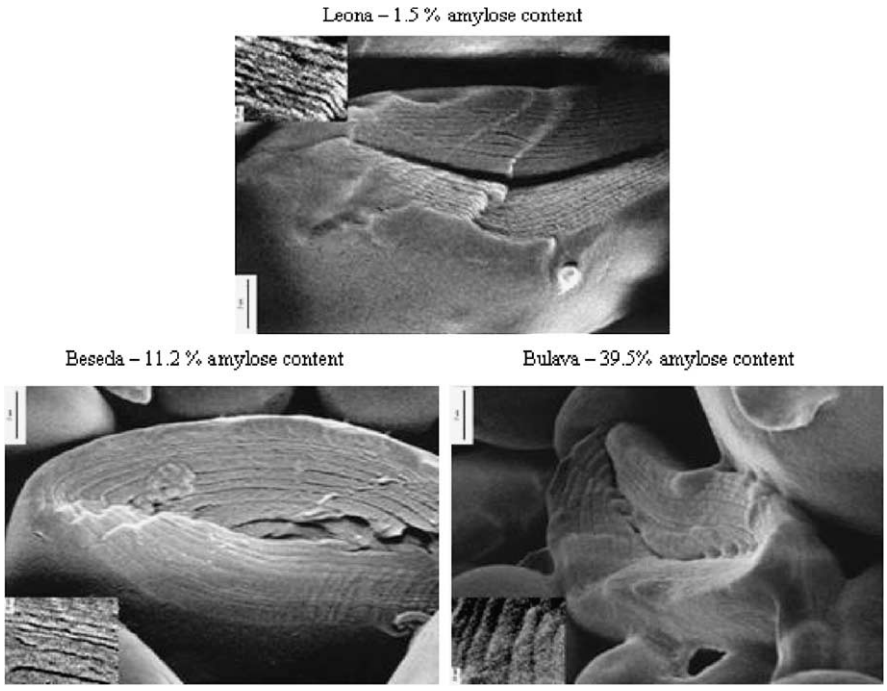

Figure 5. SEM-pictures of wheat starches with different amylose content.

Table 5. The average thickness of semi-crystalline growth rings in wheat starches with different amylose content

Starch	Amylose content (%)	Average thickness of semi-crystalline growth rings (nm)
Leona	1.5	182
Beseda	11.2	240
Bulava	39.5	312

related to semi-crystalline growth rings, the latter to amorphous background.

DIA of the SEM photographs (Table 5, Fig. 5) show that the average thickness of semi-crystalline growth rings is, generally, in agreement with the earlier published data[3,18] on growth rings in starches from other origins. Detailed analysis of the data (Table 5) shows that the average thickness of semi-crystalline growth rings increases, rather regularly, with increasing amylose content. In other words, the largest thickness of semi-crystalline growth ring is observed in wheat starches with larger amylose content (Fig. 5, Table 5).

Comparing the published data[3,18] with those in the present work, it is possible to suggest that the internal structure of starch granules is dependent not only on the botanical origin of the starch but also on the amylose content.

4. Conclusions

The structural characteristics of wheat starches with different amylose content were studied with SAXS and SEM methods. These studies provided additional information about the macromolecular organization of starch polysaccharides. A noteworthy result is the role of the amylose content on the average thickness of semi-crystalline growth rings in a given starch species. The SAXS data obtained show that an increase of amylose content in native wheat starches is accompanied by a decrease of the electron density contrast between crystalline and amorphous lamellae whilst their thickness and the overall cluster size remains unchanged. The decrease of the electronic density contrast appears related to an accumulation of defects, particularly, amylose tie-chains. The data obtained allow a tentative explanation for the decrease in the melting temperature of wheat starches on the increasing of amylose content, although a definite conclusion cannot yet be assessed owing to many questions that still remain open and demand additional investigation.

Acknowledgements

The authors thank N. S. Eiges, L. I. Weisfeild, and V. A. Volcheck for supplying wheat samples of different varieties, as well as Prof. P. Seib for supplying by the waxy wheat starch. Experimental work was done with the partial financial support of the Division of Chemistry and Science of Materials of Russian Academy of Sciences (Programme N6, 2003) and with the support of a joint grant from the Russian Ministry of Industry, Science and Technology and the Italian Ministry of Foreign

Affairs (Executive routine of third mixed session of Russian–Italian commission on scientific and technical cooperation for 2003–2004 years signed in Rome by October 17, 2002, Appendix 3. Number 69AG2).

References

1. Robin, J. P.; Mercier, C.; Charbonniere, R.; Guilbot, A. *Cereal Chem.* **1974**, *51*, 389–406.
2. Manners, D. J. *Carbohydr. Polym.* **1989**, *11*, 87–112.
3. Waigh, T.; Donald, A. M.; Heidelbach, F.; Riekel, C.; Gidley, M. J. *Biopolymers* **1999**, *49*, 91–105.
4. Jenkins, P. J.; Cameron, R. E.; Donald, A. M. *Starch/Stärke* **1993**, *45*, 417–420.
5. Jenkins, P. J.; Donald, A. M. *Int. J. Biol. Macromol.* **1995**, *17*, 315–321.
6. Donald, A. M.; Kato, K. L.; Perry, P. A.; Waigh, T. A. *Starch/Stärke* **2001**, *53*, 504–512.
7. Pikus, S.; Jamroz, J.; Kobylas, E.; Wlodarczyk, M.; Bogdanowicz, T. In *Conference Proceedings. Tenth International Starch Convention*. Cracow (Poland), June 11–14, 2002; p 72.
8. Yuryev, V. P.; Wasserman, L. A.; Andreev, N. R.; Tolstoguzov, V. B. In *Starch and Starch Containing Origins—Structure, Properties and New Technologies*; Yuryev, V. P., Cesaro, A., Bergthaller, W., Eds.; Nova Science: New York, 2002; Chapter 2, pp 23–56.
9. Matveev, Yu. I.; Elankin, N. Yu.; Kalistrova, E. N.; Danilenko, A. N.; Niemann, C.; Yuryev, V. P. *Starch/Stärke* **1998**, *50*, 141–147.
10. Graybosch, R. A. *Trends Food Sci. Technol.* **1998**, *9*, 135–142.
11. Yuryev, V. P.; Eiges, N. S.; Wasserman, L. A.; Bocharnikova, I.; Belousova, E. M. In *Russia—Cereal Power*; Pischepromizdat: Moscow, 2003; pp 109–112.
12. Bocharnikova, I.; Wasserman, L. A.; Krivandin, A. V.; Fornal, J.; Blaszczak, W.; Chernykh, V. Y.; Schilardi, A.; Yuryev, V. Pa. *J. Therm. Anal. Calorim.* **2003**, *74*, 681–689.
13. Vasanthan, T.; Bhatty, R. S. *Cereal Chem.* **1996**, *73*, 199–207.
14. Zobel, H. F. *Starch/Stärke* **1988**, *40*, 1–7.
15. Wang, T. L.; Bogracheva, T. Ya.; Hedley, C. L. *J. Exp. Bot.* **1998**, *49*, 481–502.
16. Eliason, A.-C.; Larson, K. *Cereals in Breadmaking*; Marcel Dekker: New York, 1993; Chapter 2, pp 96–129.
17. Baker, A. A.; Miles, M. J.; Helbert, W. *Carbohydr. Res.* **2001**, *330*, 249–256.
18. Ridout, M. J.; Gunning, A. P.; Parker, M. L.; Wilson, R. H.; Morris, V. J. *Carbohydr. Polym.* **2002**, *50*, 123–132.
19. Eiges, N. S. In *Starch and Starch Containing Origins—Structure, Properties and New Technologies*; Yuryev, V. P.; Cesaro, A., Bergthaller, W., Eds.; Nova Science: New York, 2002; Chapter 26, pp 361–373.
20. Richter, M.; Augustadt, S.; Schierbaum, F. *Ausgewahlte Methoden der Stärkechemie*; VEBFachbuch: Leipzig, 1968.
21. Franks, A. *Brit. J. Appl. Phys.* **1958**, *9*, 349–352.
22. Cheremukina, G. A.; Chernenko, S. P.; Ivanov, A. B.; Pashekhonov, V. D.; Smykov, L. P.; Zanevsky, Yu. V. *Isotopenpraxis* **1990**, *26*, 547–549.
23. Shedrin, B. M.; Feigin, L. A. *Kristallografia* **1966**, *11*, 159–163.
24. Hosemann, R.; Bagchi, S. N. *Direct Analysis of Diffraction by Matter*; Noth-Holland: Amsterdam, 1962.
25. Vainshtein, B. K. *Diffraction of X-Rays by Chain Molecules*; Elsevier: Amsterdam, 1966.
26. Feigin, L. A.; Svergun, D. I. *Structure Analysis by Small-Angle X-Ray and Neutron Scattering*; Plenum: New York, 1987.
27. Buttrose, M. S. *Starch/Stärke* **1963**, *15*, 85–92.
28. Waigh, T. A.; Kato, K. L.; Donald, A. M.; Gidley, M. J.; Clarke, Ch. J.; Riekel, C. *Starch/Stärke* **2000**, *52*, 450–460.
29. Gidley, M. J. Personal communication, 1995; reference quoted from Ref. 5.
30. Kozhevnikov, G. O.; Protserov, V. A.; Wasserman, L. A.; Pavlovskaya, N. E.; Golischkin, L. V.; Milyaev, V. N.; Yuryev, V. P. *Starch/Stärke* **2001**, *53*, 201–210.
31. Protserov, V. A.; Karpov, V. G.; Kozhevnikov, G. O.; Wasserman, L. A.; Yuryev, V. P. *Starch/Stärke* **2000**, *52*, 461–466.
32. Yuryev, V. P.; Wasserman, L. A. In *Biochemistry and Chemistry: Research and Developments*; Zaikov, G. E., Lobo, V. M. M., Eds.; Nova Science: New York, 2003; Chapter 7, pp 91–113.
33. Bershtein, V. A.; Egorov, V. M. In *Differential Scanning Calorimetry of Polymers. Physics, Chemistry, Analysis, Technology*; Kemp, T. J., Ed.; Ellis Horwood: New York–London–Toronto–Sydney–Singapore, 1994, 253p.
34. Kalichevsky, M. T.; Ring, S. G. *Carbohydr. Res.* **1987**, 323–328.
35. German, M. L.; Blumenfield, A. L.; Guenin, Ya. V.; Yuryev, V. P.; Tolstoguzov, V. B. *Carbohydr. Polym.* **1992**, *18*, 27–34.
36. Koz'mina, N. P. *Zernovedenie*; Zagotizdat: Moscow, 1955.
37. Wasserman, L. A.; Eiges, N. S.; Koltysheva, G. I.; Andreev, N. R.; Karpov, V. G.; Yuryev, V. P. *Starch/Stärke* **2000**, *53*, 629–634.
38. Kiseleva, V. I.; Tester, R. F.; Wasserman, L. A.; Krivandin, A. V.; Popov, A. A.; Yuryev, V. P. *Carbohydr. Polym.* **2003**, *51*, 407–415.
39. Matveev, Y. I.; Soest, J. J. G.; Niemann, C.; Wasserman, L. A.; Protserov, V. A.; Ezernitskaja, M.; Yuryev, V. P. *Carbohydr. Polym.* **2001**, *44*, 151–160.
40. Sharples, A. *Introduction to Polymer Crystallisation*; Edward Arnold Ltd.: London, 1966.